

Design of hard-target penetrator nose geometry in the presence of high-speed, velocity-dependent friction, including the effects of mass loss and blunting

A. M. Neely-Horton, R. N. Davis & S. E. Jones
*Department of Aerospace Engineering and Mechanics,
The University of Alabama*

Abstract

A new analytical model for high-speed, velocity-dependent friction was developed and successfully applied to the problem of one-dimensional, hard-target penetration by a number of high-strength steel, ogive-nosed penetrators [1]. Resulting predictions of penetrator performance and target strength deduced from the model were very consistent and correlated well with previously reported experimental data. Implementation of the mathematical model was subsequently simplified by the development of a stepwise, incremental approximation of the velocity-dependent coefficient of sliding friction [2]. This modification preserved the quality of the linear approximation to the observed velocity dependence in sliding friction at high speeds, while making the model much more practical for engineering applications [3]. These results are now applied to penetrator nose geometries other than the ogival case, and the effects of blunting and progressive mass loss from the nose are considered. By incorporating the effects of the changing penetrator nose mass and geometry due to frictional wear during the penetration event [4], it becomes possible to use the model to design the optimal geometry for a hard-target penetrator nose to maximize penetration depth under specified conditions of penetrator material, impact velocity, and target strength. The results of the analysis are applied to a number of cases in which data for hard-target penetration has been reported. *Keywords: hard-target penetration, high-speed friction, nose erosion, optimal nose geometry.*



1 Introduction

A long-standing difficulty in high-speed penetration problems is the assumed velocity-dependence in sliding friction (see Kragelskii [5]). Contemporary work has often been forced to explain penetrator performance by changing the target strength factor R , which should be a constant. Jones, et al [1] developed a new friction law that included a free parameter, the critical velocity u , as a function of penetrator performance. This critical velocity is seen to govern the reduction in the coefficient of sliding friction μ at increasing sliding speed. These and other results obtained using subsequent developments of the new analytical model [2,3,6] were highly successful at explaining and predicting penetrator behaviour. Davis, et al [4] then developed a method to predict mass loss and blunting of high-speed penetrators, including non-ogival cases, which will now be used in this paper to determine the optimal nose geometry for a high-speed penetrator to maximize penetration depth.

2 Computer modelling of nose erosion

Davis, et al [4] non-dimensionalized the shank radial distance r and the axial coordinate x according to $\varphi = r/a$ and $\xi = x/b$, and for a generalized, dimensionless nose equation implemented:

$$\varphi = \frac{\xi^n}{\alpha^n} \left(c_0 + \frac{c_1}{\alpha} \xi + \frac{c_2}{\alpha^2} \xi^2 \right) \quad (1)$$

where the free parameters governing the geometry are n , c_0 , c_1 , and c_2 . The exponent n governs the degree of blunting of the nose and must be a positive, real number. In order for the nose profile to match to the shank radius at $\xi = 1$, it is the case that:

$$\frac{c_0}{\alpha^n} + \frac{c_1}{\alpha^{n+1}} + \frac{c_2}{\alpha^{n+2}} = 1. \quad (2)$$

For an ogive, $n = 1$ and the generalized, non-dimensional approximation to an ogive with calibre-radius-head (CRH) of 3.0, becomes:

$$\varphi = \xi \left(1.8 - 0.6\xi - 0.2\xi^2 \right). \quad (3)$$

Figure 1 presents the approximate nose profile for a CRH = 3.0 ogive superimposed onto an actual photograph of the penetrator nose which was utilized in order to assure proper modelling of the geometry. In designing the optimal nose geometry for a high-speed penetrator, the penetration and blunting algorithms[2,4] will be applied to the general nose equation (1) for various values of n , c_0 , c_1 , and c_2 (describing multiple possible nose geometries), and the relative performance of the various geometries evaluated.



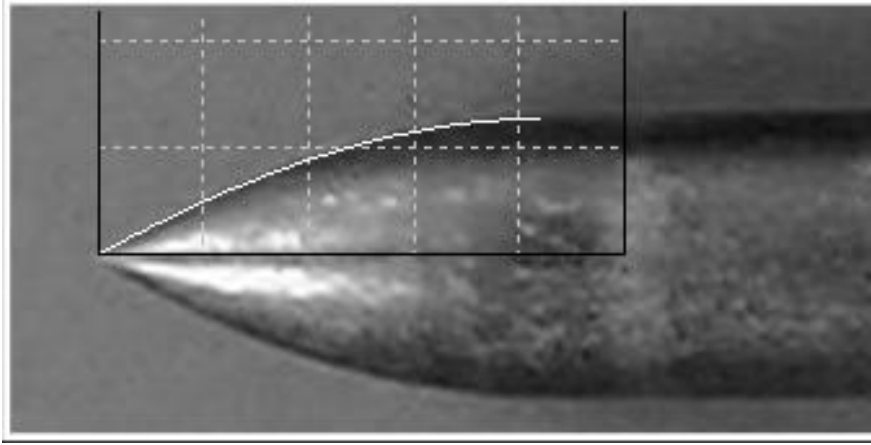


Figure 1: CRH=3.0 nose profile approximated by general nose equation, superimposed against actual CRH=3.0 penetrator nose.

3 Nose geometry design for optimal penetration

In order to obtain the geometric design for optimal penetration with the inclusion of mass loss effects, the four free parameters presented in the general nose equation (1) were iteratively included in the fore-mentioned computer model. This study was performed for a range of impact velocities from 800 m/s to 1600 m/s. So as to establish a comparative basis, experimental parameters taken from the data reported by Jerome, et al [7] were kept as constants during this analysis. Throughout the optimization process a listing of penetration depths and correlating geometric coefficients was maintained and utilized in final selection of the optimum parameters. Such data for the bluntness parameter, n , as presented in Figure 2, clearly defines an upper limit corresponding to maximum penetration depth.

All analyses produced the general nose shape described by a bluntness parameter centring on 0.72 which is highly comparable to that geometry developed by Jones and Rule [8]. The three remaining free parameters were as well optimized and incorporated into the general nose equation, given in equation (4), thus producing the description of the optimal nose geometry for attaining maximum penetration depth for the target parameters used in the model.

$$\varphi = \xi^{0.72} (0.94 + 0.01\xi + 0.05\xi^2) \quad (4)$$

The resulting nose profile is shown in Figure 3 accompanied with a graphical overlay of the above prescribed equation.



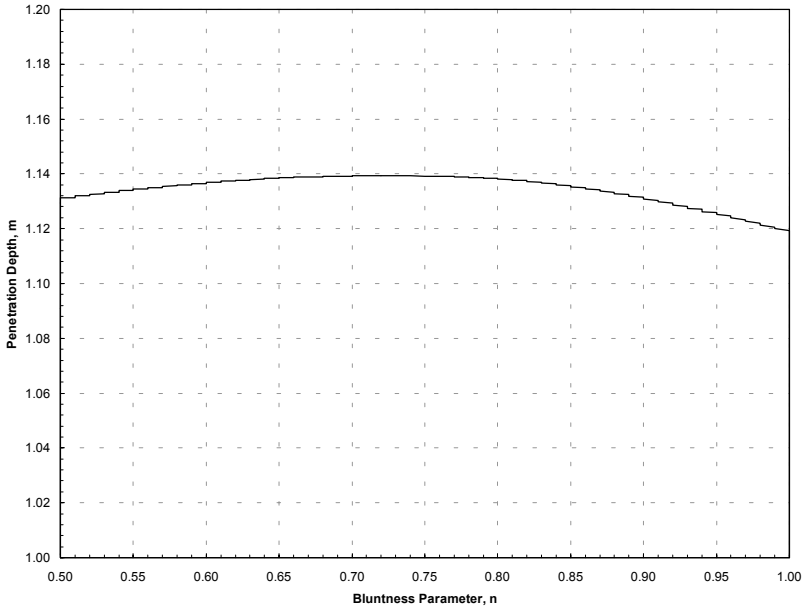


Figure 2: Optimization of Bluntness Parameter at an impact velocity = 1600 m/s.

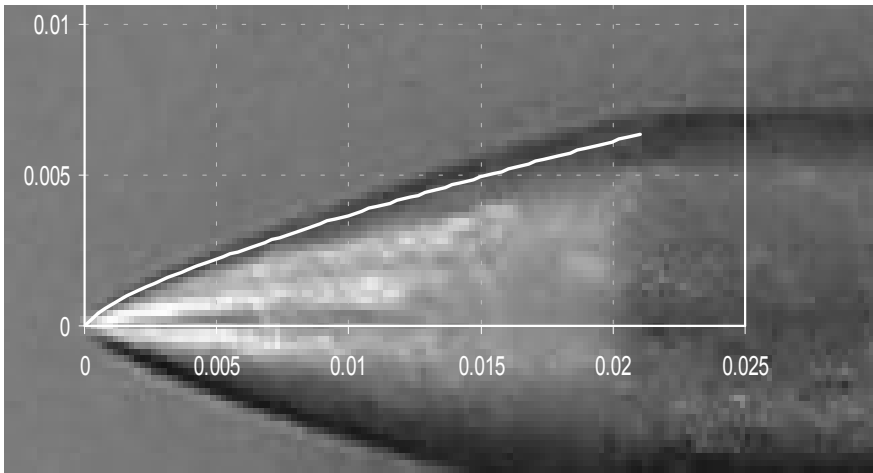


Figure 3: Optimal nose geometry profile correlating to maximum penetration.



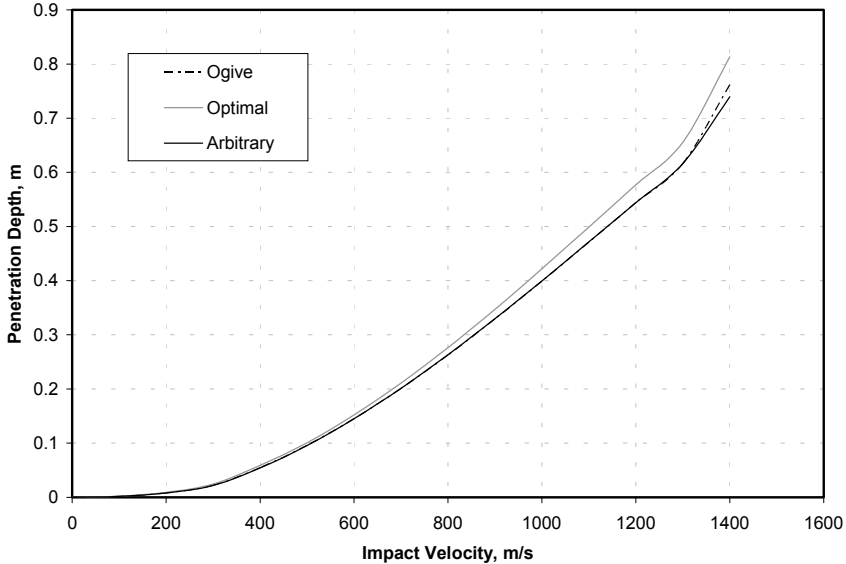


Figure 4: Penetration depth based on impact velocity for the ogive, optimal and sub-optimal nose geometry.

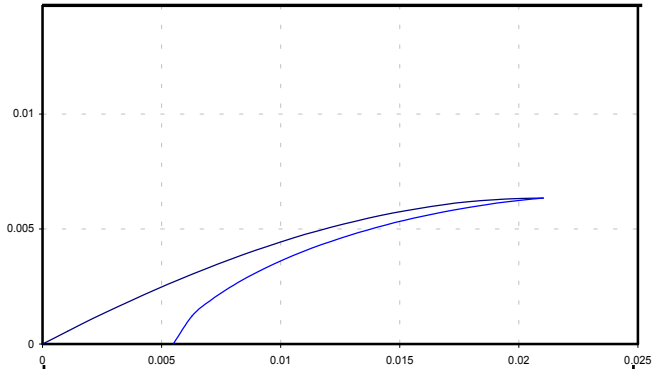
To supplement the analysis encompassing this optimization technique, secondary runs were performed with the code incorporating four fixed parameters correlating to three nose geometries: the standard ogival nose, the above described optimal geometry, and a sub-optimal geometry having a bluntness parameter of 0.5. Penetration depth predictions were generated for the three nose shapes and are presented in Figure 4. This comparison clearly illustrates a distinct performance increase in the optimal geometry as compared to the ogival nose shape.

4 Relationship between mass loss and penetration depth

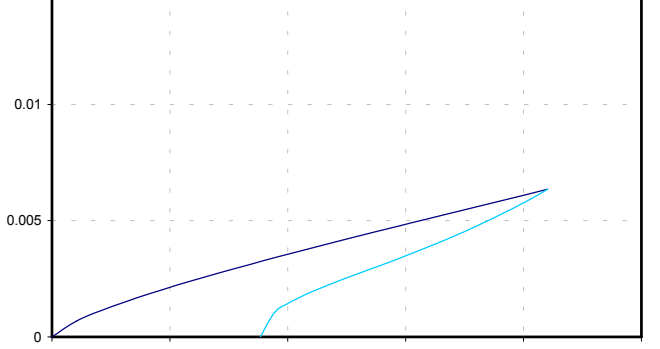
Reported mass loss data that was previously utilized in studies was generally calculated from the weights of recovered penetrators. However, with nontrivial accretion of lost nose mass to the shank, it is clear that measurement of final weight will frequently underestimate the mass actually lost from the nose. Furthermore, the high degree of scatter that is typical of reported mass loss data indicates the presence of other difficulties, such as mass loss due to friction acting on the shank of the projectile due to elastic unloading of the target. Consequently, previous work sought to fit the generalized nose equation (1) against photographs of eroded noses using appropriate values of n , c_0 , c_1 , and c_2 . When these equations describing final nose geometry were used to calculate the nose volume, and the change in nose volume was used to determine mass loss (assuming constant penetrator density), the discrepancy with reported mass loss data was clear, and a strong case made for using mass losses calculated from nose volume change.



Ogive Nose



Optimal Nose



Sub-Optimal Nose

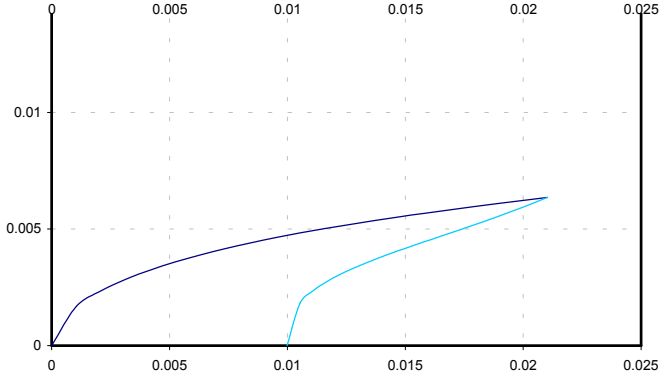


Figure 5: Profile of initial nose geometry for three high-strength steel penetrators and predicted profile after a penetration event corresponding to an impact velocity of 1400 m/s.

For this paper, mass losses for the non-ogival cases being evaluated were determined using this same technique of calculated volume change. Figure 5 illustrates the final erosion geometries obtained through predictions on the three previously analyzed nose geometries. Generally it has been thought that



minimizing the wear would serve to maximize penetration depth. In comparing these new results, however, it was determined that minimum mass loss does not, in fact, correlate with maximum penetration depth. Instead, it is clear that the decisive factors in penetrator performance are the actual set of mechanisms for mass loss that are acting on a given penetrator—for example, surface melting of the nose, removal of surface asperities by grinding, etc.—and the relative effectiveness of these processes for a given penetrator material and nose geometry.

In order to validate these conclusions regarding the relationship between mass loss and penetration depth, penetration experiments were conducted under controlled, laboratory conditions. Penetrators fired included one of the geometry presented in this paper as optimal and one with calibre-radius-head (CRH) of 3.0. The optimal penetrator achieved the greater penetration depth, as expected (and corresponding closely to the performance predicted by the computer model), in spite of undergoing greater mass loss. These results are being further studied and future work in this area will be forthcoming.

5 Conclusions

The results of an analytical model of high-speed, velocity-dependent friction are now applied to penetrator nose geometries other than the ogival case, and the effects of blunting and progressive mass loss from the nose are considered. With the incorporation of a non-dimensional nose equation into the model, the capability to represent the effects of changing penetrator nose geometry and mass and due to frictional wear during the penetration event became possible. Based on these advancements, an optimization of the nose geometry for a hard-target penetrator was sought in order to maximize penetration depth under specified conditions of penetrator material, impact velocity, and target strength. This analysis resulted in definition of an optimal nose shape with which penetration depth is maximized.

An additional concept was presented questioning the validity in the correlation between minimal mass loss and maximum penetration depth. When analysis was performed on the mass loss of the determined optimal and ogival nose shape, it was found that penetration depth can not, in fact, be maximized by minimal mass loss. Rather, penetration performance was found dependent on the manner in which a penetrator experiences wear.

Acknowledgments

The authors gratefully acknowledge the support of the U.S. Air Force, Munitions Directorate, Air Force Research Laboratory, Eglin AFB, FL.

References

- [1] Jones, S. E., Hughes, Mary L., Toness, Odin A., and Davis, Robert N., 2003, "A One-Dimensional Analysis of Rigid Body Penetration with



- High-Speed Friction,” *Journal of Mechanical Engineering Science, Proceedings of the Institution of Mechanical Engineers, Vol 217-Part C*, pp. 411-422.
- [2] Davis, Robert N., 2003, “Modeling of High-Speed Friction Using Multi-Step Incrementation of the Coefficient of Sliding Friction,” AIAA 54th Annual Southeastern Regional Student Conference, Kill Devil Hills, NC, March 27-28, 2003.
- [3] Davis, Robert N., Jones, S.E., and Hughes, Mary L., 2003, “High-Speed Penetration of Concrete Using a New Analytical Model of Velocity-Dependent Friction”, *Thermal-Hydraulic Problems, Sloshing Phenomena, and Extreme Loads on Structures, ASME-PVP*, (to appear).
- [4] Davis, Robert N., Neely, Amanda M., and Jones, S.E., 2003, “Mass Loss and Blunting During High-Speed Penetration,” *Journal of Mechanical Engineering Science, Proceedings of the Institution of Mechanical Engineers, Part C* (submitted for publication).
- [5] Kragelskii, I. V., 1965, *Friction and Wear*, Butterworths, Inc., Washington, DC.
- [6] Jones, S. E., Davis, Robert N., Hughes, Mary L., Toness, Odin A., 2002, “Penetration with High-Speed Friction,” *Thermal-Hydraulic Problems, Sloshing Phenomena, and Extreme Loads on Structures, PVP-Vol. 435*, F.J. Moody, ed., pp. 255-262.
- [7] Jerome, D. M., Tynon, R. T., Wilson, L. L., and Osborn, J. J., 2000, “Experimental Observations of the Stability and Survivability of Ogive-Nosed, High-Strength Steel Alloy Projectiles in Cementitious Materials at Striking Velocities from 800-1800 m/sec,” 3rd Joint Classified Ballistics Symposium, San Diego, CA, May 1-4, 2000.
- [8] Jones, S. E. and Rule, W. K., 2000, “On the Optimal Nose Geometry for a Rigid Penetrator, Including the Effects of Pressure-Dependent Friction,” *Int. J. Impact Engng.*, **24**, 403-415.
- [9] Jones, S. E., Toness, O., Jerome, D. M., and Rule, William K., 2001, “Normal Penetration of Semi-Infinite Targets by Ogive-Nose Projectiles, Including the Effects of Blunting and Erosion,” *Thermal Hydraulics, Liquid Sloshing, Extreme Loads, and Structural Response, PVP-Vol. 421*, F.J. Moody, ed., pp. 53-59.
- [10] Jones, S. E., Foster, J. C., Jr., Toness, O. A., DeAngelis, R. J., Rule, W.K., 2002, “An Estimate for Mass Loss from High Velocity Steel Penetrators,” *Thermal-Hydraulic Problems, Sloshing Phenomena, and Extreme Loads on Structures, PVP-Vol. 435*, F.J. Moody, ed., pp. 227-237.
- [11] Klepaczko, Janusz R., 2001, “Surface Layer Thermomechanics of Steel Penetrators at High and Very High Sliding Velocities,” Technical Report, University of Florida, GERC, Shalimar, Florida.
- [12] Tate, A., 1967, “A Theory for the Deceleration of Long Rods after Impact,” *J. Mech. Phys. Solids*, **15**, pp. 387-399.

